

## REFLECTARRAYS OF RECTANGULAR MICROSTRIP PATCHES FOR DUAL-POLARIZATION DUAL-BEAM RADAR INTERFEROMETERS

S. R. Rengarajan\*

Department of Electrical and Computer Engineering, California State University, Northridge, CA 91330-8346, USA

**Abstract**—Microstrip reflectarrays consisting of rectangular patches are investigated for application in space-based dual-polarized dual-beam radar interferometers. For nadir looking beams the angle of incidence of feed radiation in each patch is nominally  $45^\circ$ . In such an application, square-patch reflectarrays can be designed for only one polarization with a sacrifice in performance in the other whereas reflectarrays consisting of rectangular patches may be designed for both polarizations, thereby improving their radiation performance. Piecewise planar parabolic reflectarrays consisting of square patches exhibit poor scan performance in tilted configuration. It is shown that with the use of rectangular patches in such a reflectarray one can design two beams of different polarizations for two offset feeds, thereby providing significant improvement in bandwidth and radiation performance.

### 1. INTRODUCTION

Microstrip reflectarray antennas find applications in space based radars because of their low profile and ease of design, manufacture, and deployment. Pozar et al. have presented the analysis and synthesis of reflectarrays consisting of variable size square patches using the infinite array model [1]. Dual-polarized dual-beam reflectarrays consisting of square patches and fed by slot arrays have been discussed previously [2, 3]. Esteban-Fernandez et al. have proposed similar antenna geometry for the Surface Water and Ocean Topography (SWOT) mission at Ka band [4]. Encinar and Barba reported a two-layer reflectarray of rectangular patches for producing two beams, one

---

*Received 16 September 2011, Accepted 15 October 2012, Scheduled 16 October 2012*

\* Corresponding author: Sembiam Rajagopal Rengarajan (srengarajan@csun.edu).

at 20 GHz in horizontal polarization and the other at 30 GHz in vertical polarization [5]. Encinar et al. designed a reflectarray to produce two contour beams, one horizontally polarized for the European coverage and the other vertically polarized for the coverage of the eastern United States [6]. Roederer patented a piecewise planar parabolic reflectarray (PPPR) [7] while Legay et al. mention the use of PPPR in a recent paper [8]. Racette et al. employed a cylindrical parabolic reflectarray in dual-frequency radar [9]. Hodges and Zawadzki found that a reflectarray consisting of piecewise planar square-patch panels mimicking a parabolic cylinder in a tilted configuration had excessive scan loss [2] and therefore they used a fully planar reflectarray for wide swath ocean altimetry (WSOA).

Two objectives of this paper are concerned with reflectarrays for nadir looking dual-polarization dual-beam radar interferometers, such as the WSOA [2]. First, it will be shown that for a fully planar reflectarray, the use of rectangular patches improves the gain by 0.3 to 0.5 dB over the square patch array counterparts. Future space based interferometric radars with nadir looking dual polarized dual beams will require ever increasing aperture sizes. Offset parabolic reflectors are not suited to such systems because of their poor beam scan performance with displaced feeds. Fully planar microstrip reflectarrays exhibit good scan performance but they have severe bandwidth limitation for large apertures because of the modulo  $2\pi$  phase correction employed in the design of reflectarrays. PPPR will obviate this bandwidth limitation. Hodges and Zawadzki found that the symmetric arrangement of PPPR leads to increased mass and moment of inertia, and limits the ability to control the center of gravity of the instrument. The offset tilted PPP reflectarray was proposed to improve the spacecraft accommodation of the WSOA but it exhibits poor scan performance [2]. With the use of rectangular patches in a tilted PPPR, dual polarized dual beams can be designed for two feeds without the need for scan. The second objective of this paper is to demonstrate the excellent pattern and bandwidth performance (bandwidth limited by the patch resonance only) of PPPR employing rectangular patches.

The receive mode design technique presented in [10] is extended in the design of fully planar and PPP rectangular patch arrays in this paper. This method is substantially faster and more accurate than the conventional transmit mode design technique, especially for large arrays with tens of thousands of patches. The key component of our design and analysis methodology is our moment method code for an infinite array of patches excited by a plane wave which was previously validated against the commercial finite element code HFSS as well as

waveguide simulator experimental data [11]. Our design and analysis codes were validated previously by comparing our results with those of Pozar [1, 10]. In addition, our results matched those of [2] for fully planar square patch reflectarrays, further validating the procedure used in this paper.

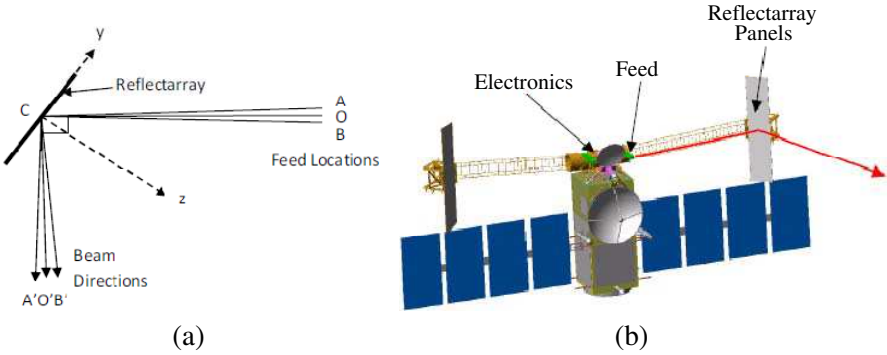
## 2. FULLY PLANAR REFLECTARRAY

Figure 1 shows the geometry of an offset reflectarray and beam positions for different feed locations for an application such as the dual beam dual polarization nadir looking radar antenna used in interferometric mapping application WSOA [2]. We consider a reflectarray of size 2.145 m in the  $x$ -direction and 0.5 m in the  $y$ -direction, tilted at  $45^\circ$  with respect to the vertical, consisting of  $190 \times 44$  patches with a lattice spacing of  $0.5\lambda$ , where  $\lambda$  is the free space wavelength at 13.285 GHz. The substrate material is 32 mil (0.81 mm) thick Rogers RO4003 of  $\epsilon_r = 3.38$ . The nominal feed location,  $O$  is 2.145 m away from the reflectarray center  $C$ . For a feed located at  $O$ , a nadir looking beam along  $O'$  will result if the reflection phase from each patch is designed for proper collimation. When a horizontally polarized (hpol) feed is located at  $A$ , and a vertically polarized (vpol) feed is at  $B$ , the corresponding beams will be along  $A'$  and  $B'$  respectively. In interferometric radar mapping applications each beam is offset from the nadir direction by about one beamwidth. The second reflectarray will have its vpol feed above and the hpol feed below [2, 4]. The scan performance in this case is excellent and the beam deviation factor is expected to be close to one, since the equivalent  $f/D$  ratio is large [12].

A feed model in the form of  $\cos^q \theta$  was found to be not optimum for a rectangular aperture, even if we use different  $q$  values in the two principal planes. Slot array feeds similar to those in [2, 3] were used to provide about  $-10$  dB edge taper. For hpol, a  $3 \times 13$  array was used with element spacing of  $0.66\lambda$  and  $0.74\lambda$  in the horizontal and vertical directions respectively. A  $3 \times 16$  array with spacing of  $0.65\lambda$  and  $0.73\lambda$  was used for vpol. The aperture distribution was uniform in the vertical direction for both feeds whereas the horizontal distribution was 0.5, 1, 0.5 for hpol and 0.63, 1, 0.63 for the vpol. No attempt was made to shape the feed pattern to maximize the efficiency of the reflectarray.

### 2.1. Reflectarrays of Square Patches

The reflectarray geometry shown in Fig. 1(a), consisting of square patches was designed using the receive mode design technique [10] for



**Figure 1.** Dual-beam nadir looking radar antenna. (a) Feed locations and beam directions of an offset reflectarray. (b) WSOA reflectarray antenna from [2].

hpol feed located at  $O$ . The reflection phase data for a set of values of the size of the square patch, ‘ $a$ ’ embedded in an infinite array of identical elements were computed using the moment method [11] for an incident plane wave arriving from  $\theta = 45^\circ$  and  $\phi = -90^\circ$ . In the design, the required size  $a_n$  for patch  $n$  is interpolated from the computed phase data such that the sum of the phase of the incident plane wavefront at patch  $n$ ,  $\phi_{wn}$  and the reflection phase of patch  $n$ ,  $\phi_{rn}$  is the conjugate of the phase of the feed radiation at patch  $n$ ,  $\phi_{fn}$  [10].

i.e.,

$$\phi_{wn} + \phi_{rn} = -\phi_{fn} \quad (1)$$

Once the reflectarray is designed, the transmit mode analysis [10] is employed to compute the gain and obtain radiation patterns for different locations of hpol and vpol feeds using equivalent electric and magnetic currents. The equivalence principle formulation employing electric and magnetic currents is found to be more accurate [13] than the one using electric currents only [1]. The locations  $A$  and  $B$  are approximately 12.5 cm from  $O$  so that the two beams along  $A'$  and  $B'$  are approximately  $\pm 3.3^\circ$  (one beamwidth in the  $yz$  plane) away from the nadir direction. When the feed is located at  $A$  or  $B$  its beam peak is tilted slightly with respect to the direction  $OC$  so that the illumination levels at the two edges in the  $yz$  plane are the same. Table 1 shows the gain values in dB for different feed locations.

For the case of hpol feed at  $O$  the computed gain is 40.5 dB. The aperture size is  $2091.6\lambda^2$ . Since the beam is pointing at  $45^\circ$  with respect to the array normal the projected area is reduced by a factor of 0.707, thereby reducing the effective aperture by 1.5 dB. Therefore

**Table 1.** Gain in dB of the square patch reflectarray designed for hpol for each feed location and polarization.

Feed polarization	Feed at $O$	Feed at $B$	Feed at $A$
hpol	40.50	40.70	40.20
vpol	40.19	40.48	39.72

**Table 2.** Gain in dB of the rectangular patch reflectarray.

Feed polarization	Feed at $O$	Feed at $B$	Feed at $A$
hpol	40.53	40.72	40.22
vpol	40.55	40.78	40.18

the maximum directivity is 42.69 dB and the realized value of 40.5 dB represents 60.4% efficiency. For a feed located at  $B$  there is an increase in gain of about 0.2 dB whereas for a feed at  $A$  the gain dropped relative to the nadir beam by about 0.3 dB. These results are consistent with the fact that the projected aperture for the  $41.7^\circ$  beam increases by 0.24 dB with respect to the  $45^\circ$  beam whereas for the  $48.3^\circ$  beam it drops by 0.265 dB. The gain value for the vpol feed is on an average 3.3 dB below that of the hpol feed. The reflectarray designed for hpol is expected to exhibit a suboptimal performance for the vpol since the reflection phase of vpol differs from that of hpol as shown in Fig. 2. The range for phase data is less than the desired  $360^\circ$  in Fig. 2 as well as for all other cases for the reflectarrays considered in this paper, thereby resulting in a small error. For a reflectarray designed for vpol, calculated gain values for different feed locations and polarizations showed results similar to those in Table 2, with greater values for the vpol feeds.

## 2.2. Design of Rectangular Patch Array for a Feed at $O$

Rectangular patches have two degrees of freedom and therefore it is possible to design a reflectarray for a feed at  $O$  polarized in the vertical as well as in the horizontal direction. Let  $\phi_{rh}$  be the reflection phase for an hpol plane wave from  $\theta = 45^\circ$ ,  $\phi = -90^\circ$  incident at a rectangular patch of dimensions  $(a, b)$  where  $a$  and  $b$  are the horizontal and vertical dimensions respectively.  $\phi_{rv}$  is the corresponding reflection phase value for a vpol wave. For a given value of the phase  $\psi$  the range  $(-180^\circ, 180^\circ)$ , we find initial values  $(a, b)$  from the results of square patches as follows.

$$\phi_{rh}(a, a) = \phi_{rv}(b, b) = \psi \quad (2)$$

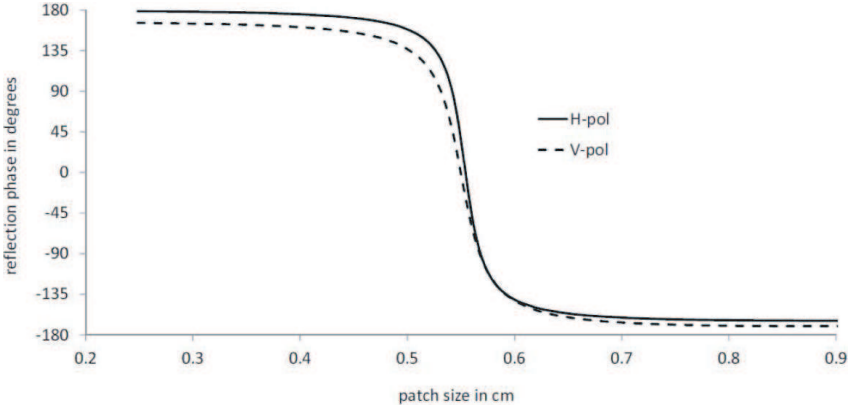


**Figure 2.** The reflection phase versus the size of square patches for hpol and vpol for a plane wave incident from  $\theta = 45^\circ$  and  $\phi = -90^\circ$ .

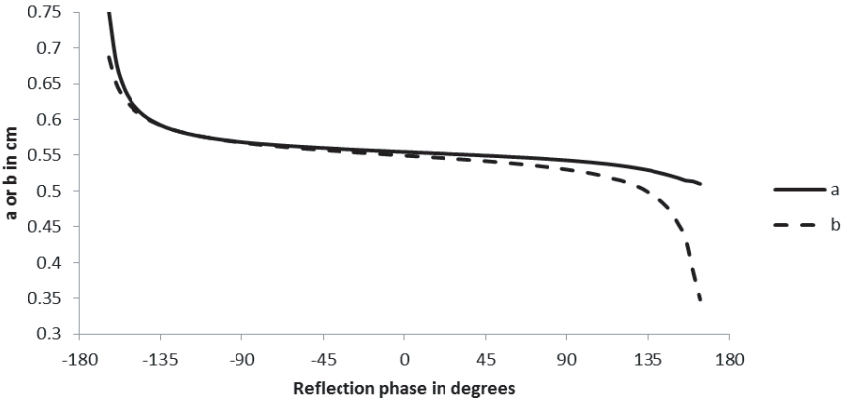


**Figure 3.** Rectangular patch dimensions ( $a$ ,  $b$ ) for a given value of the reflection phase  $\psi$  or both polarizations that minimizes error in (3).

Subsequently we evaluate the rectangular patch size ( $a$ ,  $b$ ) by minimizing the error term in (3) using the reflection phase data computed from the moment method [11].

$$e = [\phi_{rh}(a, b) - \psi]^2 + [\phi_{rv}(a, b) - \psi]^2 \quad (3)$$

The values of  $a$  and  $b$  obtained by this procedure for different  $\psi$  values are plotted in Fig. 3. The dimensions ( $a_n$ ,  $b_n$ ) of the patch  $n$  are obtained by two one-dimensional interpolations of curves shown in Fig. 3 such that Eqn. (4) is satisfied. Design Eqn. (4) is similar to (1) but accounts for both polarizations.

$$\phi_{rh}(a_n, b_n) = \phi_{rv}(a_n, b_n) = -\phi_{fn} - \phi_{wn} = \psi_n \quad (4)$$

Table 2 shows computed gain values for different feed locations and polarizations for the reflectarray designed using Eqn. (4). The gain is nearly independent of polarization and it depends only on the feed location. The vpol results of Table 2 are improved by an average of 0.37 dB with respect to those in Table 1. Thus fully planar reflectarrays of rectangular patches exhibit superior characteristics than those of square patches.

### 2.3. Design of Rectangular Patch Array for Feeds at $A$ and $B$

Rectangular patch arrays may also be designed for two simultaneous feed locations, e.g., hpol feed at  $A$  and the vpol feed at  $B$ . An hpol plane wave is incident from  $\theta = 48.3^\circ$  and  $\phi = -90^\circ$  at a patch while a vpol plane wave is incident from  $\theta = 41.7^\circ$  and  $\phi = -90^\circ$ . We obtain a set of values of patch sizes  $(a_{ij}, b_{ij})$  for a set of phase values  $(\phi_{rh} = \psi_i, \phi_{rv} = \psi_j)$ , each of the two reflection phase values in increments over the  $360^\circ$  range, by minimizing the error in (5).

$$e(a_{ij}, b_{ij}) = (\phi_{rh} - \psi_i)^2 + (\phi_{rv} - \psi_j)^2 \quad (5)$$

This is an intensive computational process since we use the moment method code in this error minimization process. Subsequently a two-dimensional interpolation technique is used to determine the dimensions of patch  $n$ ,  $(a_n, b_n)$  that satisfies simultaneously the pair of design equations in (6).

$$\phi_{rh}(a_n, b_n) = -\phi_{fhn} - \phi_{whn} \quad (6a)$$

$$\phi_{rv}(a_n, b_n) = -\phi_{fvn} - \phi_{wvn} \quad (6b)$$

In the above equation,  $\phi_{fhn}$  and  $\phi_{fvn}$  represent the phases of the hpol and vpol feed radiations at the patch  $n$  respectively while  $\phi_{whn}$  and  $\phi_{wvn}$  are the incident hpol and vpol plane wavefront phases at patch  $n$  respectively. After completing the design we analyzed the reflectarray with an hpol feed at  $A$  and a vpol feed at  $B$ . Subsequently the design and analysis were repeated for a vpol feed at  $A$  and an hpol feed at  $B$ . The results in Table 3 show that there is no significant improvement in using this design method over the method discussed in 2.2, with results shown in Table 2, since the scan performance of this reflectarray is very good.

## 3. PIECEWISE PLANAR PARABOLIC REFLECTARRAY

The bandwidth of operation of a reflectarray is limited by two factors, the element resonance and the aperture size, the latter

**Table 3.** Gain in dB of the rectangular patch reflectarray designed for two simultaneous offset feeds at  $A$  and  $B$ .

Feed polarization	hpol at $A$ vpol at $B$	vpol at $A$ hpol at $B$
hpol	40.24	40.75
vpol	40.82	40.23

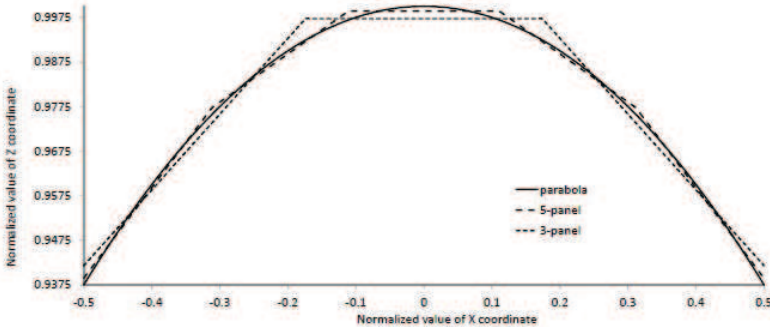


**Figure 4.** PPRR and a parabolic cylinder, in  $xz$  plane.

due to the modulo  $2\pi$  phase correction [14]. Increased values of element bandwidth may be achieved by using two-layer or three layer patches while the limitation imposed by the aperture size may be obviated by employing piecewise planar parabolic patches. In this configuration, the path length differences between the feed and the collimated wavefront through different patches are minimized if the collimated beam goes through the focal line. In the untitled PPRR geometry, the angle of incidence from the feed is close to normal for all panels and therefore the reflectarray performance is less sensitive to polarization. For the geometry shown in Fig. 1 we obtained two piecewise planar parabolas ( $f/D = 1$ ), one with three panels and the other with five panels, to mimic a parabola in the  $xz$  plane by minimizing the distance between any point in the parabola and the corresponding point on the reflectarray by employing the well-known genetic algorithm optimization. Fig. 4 shows the section of the parabolic cylinder and the 5 panel and three panel designs in the  $xz$  plane with the coordinate origin at focus. The  $z$ -axis scale is greatly expanded to show some detail.

For the WSOA geometry discussed in this paper, the fully planar reflectarray bandwidth limited by the path length differences is 8.92%

**Table 4.** Characteristics of fully planar and PPP reflectarrays for a 5 m aperture at 35.75 GHz.

	Maximum deviation from parabola	RMS deviation	Bandwidth (180 deg. max phase error) 5 m aperture, 35.75 GHz
Fully planar reflectarray	*****	*****	1.42%
3-panel PPP	0.0022, 0.21 $\lambda$	0.001, 0.093 $\lambda$	10.8%
5-panel PPP	0.0009, 0.082 $\lambda$	0.00036, 0.034 $\lambda$	38.2%

according to the criterion specified in [14]. However, for a 5 m long aperture operating at 35.75 GHz, such as the one proposed in [4] for the SWOT system the bandwidth becomes 1.4%. In this case there is a need to use PPPR for improved bandwidth performance. Table 4 shows the characteristics of fully planar and 3-panel and 5-panel PPPR for a SWOT like system. The root mean square and the maximum deviation from the parabola are substantially smaller for the 5-panel case and therefore it yields a larger bandwidth. Design procedures discussed in 2.1 and 2.3 were applied to each of the panels of the PPPR in 3.1 and 3.2 respectively below for the electrically smaller WSOA type aperture ( $f/D = 1$ ,  $D = 2.145$  m,  $f = 13.285$  GHz) so that the computational effort is substantially reduced.

### 3.1. Reflectarrays of Square Patches

The coordinates of each panel are expressed in terms of its origin and Euler angles relative to that of the central panel or the reflectarray's main coordinate system. For a feed at  $O$ , an incident plane wave coming from  $\theta = 45^\circ$  and  $\phi = -90^\circ$  with respect to the main coordinate system is converted to a wave incident at panel  $p$  from  $(\theta_p, \phi_p)$ , the direction with respect to its coordinate system [15]. We compute five (three) sets of reflection phase data, one for each panel for plane waves incident from  $(\theta_p, \phi_p)$  on an infinite array of square patches of size  $a$ . In the design, the value of  $a_{np}$  for patch  $n$  in panel  $p$  is interpolated from computed phase data for that panel such that the sum of the phase of the incident plane wavefront at patch  $n$  in panel  $p$ ,  $\phi_{wnp}$  and the reflection phase of patch  $n$  in panel  $p$ ,  $\phi_{rnp}$  is the conjugate of the phase of the feed radiation at that patch,  $\phi_{fnp}$ .

**Table 5.** Gain in dB of the square patch PPPR designed for hpol feed at  $O$ .

Feed polarization	Feed at $O$	hpol feed at $A$ vpol feed at $B$
Hpol	40.50	37.58
Vpol	40.21	37.57

**Table 6.** Direction of radiating beam from the central panel and that of the outermost panel for the hpol feed at  $A$ .

Reflectarray	Central panel Beam direction ( $\theta$ , $\phi$ )	Outermost panel Beam direction ( $\theta$ , $\phi$ )
PPPR 3-panel	48.3°, -90°	48.29°, -90.75°
PPPR 5-panel	48.3°, -90°	48.24°, -91.9°

i.e.,

$$\phi_{wnp} + \phi_{rnp} = -\phi_{fnp} \quad (7)$$

Transformations between feed, panel, reflectarray and pattern coordinates are determined using the procedure given in [15].

For the reflectarray thus designed, radiation patterns and gain were computed using the transmit mode analysis and the gain values for different feed location and polarizations are shown in Table 5 for the 5-panel PPPR. The gain values for hpol and vpol feeds at  $O$  are similar to those in Table 1. However for offset feeds, hpol at  $A$  and vpol at  $B$ , the pattern performance is poor in the plane perpendicular to the scan plane, with a gain loss of 2.6 to 2.9 dB. Similar results were found for a 5-panel PPPR designed for vpol and for different offset feed locations and polarizations. These results are consistent with the findings of [2]. Similar results were found for 3-panel PPPR. The reason for the large amount of gain loss for one beamwidth scan in a tilted PPPR is that for an offset feed the radiation from different panels are not collimated. Table 6 shows the beam direction resulting from the central panel and the outermost panel for both the 3-panel PPPR and 5-panel PPPR. Small misalignment of the two beams in the azimuth direction causes significant gain loss since the azimuth beamwidth is very small. In the case of un-tilted PPPR and fully planar reflectarray made up of panels, for a feed offset to produce a small amount of beam scan, the beams from different panels are aligned.

Table 7 shows the relative contribution to the main beam peak from radiation from each panel. In the case of a fully planar reflectarray the contribution from each panel is nearly in phase whereas in the case

**Table 7.** Amplitude and phase of radiation from each panel along the beam peak direction for an offset feed.

Panel Number	Fully planar reflectarray	Tilted PPP 5-panel reflectarray
1	0.347, 3.3°	0.243, -95.2°
2	0.732, 0.524°	0.688, -29.37°
3	1.0, 0.0°	1.0, 0.0°
4	0.732, 0.524°	0.688, -29.37°
5	0.347, 3.3°	0.243, -95.2°

of the 5-panel PPPR, there is a significant phase difference and they don't completely add up. Similar results were found for the 3-panel PPPR.

Phase perturbation studies were performed on a reflectarray with a displaced feed, using a procedure similar to that of Baars [16]. For the WSOA type geometry it was found that the fully planar reflectarray and symmetric PPPR exhibited good scan performance whereas the tilted PPPR had poor scan performance. The radiation from outer panels was slightly offset in the azimuthal direction compared to the radiation from the central panel, thus supporting the results of Table 6. Therefore tilted PPPR are not useful in applications involving beam scanning by feed displacement.

### 3.2. Design of Rectangular Patch Array for Feeds at *A* and *B*

For an hpol feed at *A* and a vpol feed at *B*, we consider an hpol plane wave from  $(\theta_{hp}, \phi_{hp})$  incident at a patch in panel number *p* while a vpol plane wave is also incident from  $(\theta_{vp}, \phi_{vp})$ .  $(\theta_{hp}, \phi_{hp})$  and  $(\theta_{vp}, \phi_{vp})$  correspond to  $(48.3^\circ, -90^\circ)$  and  $(41.7^\circ, -90^\circ)$  respectively in the main coordinate system and they may be determined using the coordinate transformation in terms of the coordinates of panel *p* using appropriate Euler angles [15]. We obtain a set of values of patch sizes  $(a_{ijp}, b_{ijp})$  for a set of phase values  $(\phi_{rhp} = \psi_{ip}, \phi_{rvp} = \psi_{jp})$ , each of two reflection phase values in increments over the  $360^\circ$  range by minimizing the error in (8).

$$e(a_{ijp}, b_{ijp}) = (\phi_{rhp} - \psi_{ip})^2 + (\phi_{rvp} - \psi_{jp})^2 \tag{8}$$

There are five (or three) sets of such data, one for each panel. A two dimensional interpolation technique is used to determine the

dimensions of patch  $n$  in panel  $p$ ,  $(a_{np}, b_{np})$  that satisfies simultaneously the pair of design equations in (9).

$$\phi_{rhp}(a_{np}, b_{np}) = -\phi_{fhnp} - \phi_{whnp} \quad (9a)$$

$$\phi_{rvp}(a_{np}, b_{np}) = -\phi_{fvnp} - \phi_{wvnp} \quad (9b)$$

In Eqn. (9),  $\phi_{fhnp}$  and  $\phi_{fvnp}$  represent the phases of the hpol and vpol feed radiations at the patch  $n$  in panel  $p$  respectively while  $\phi_{whnp}$  and  $\phi_{wvnp}$  are the incident hpol and vpol plane wavefront phases at that patch respectively. A similar procedure was used to design a reflectarray with vpol feed at  $A$  and hpol feed at  $B$ . The gain values computed for these two antennas shown in Table 8 for the five-panel PPPR are found to be slightly better than those in Tables 2 and 3,

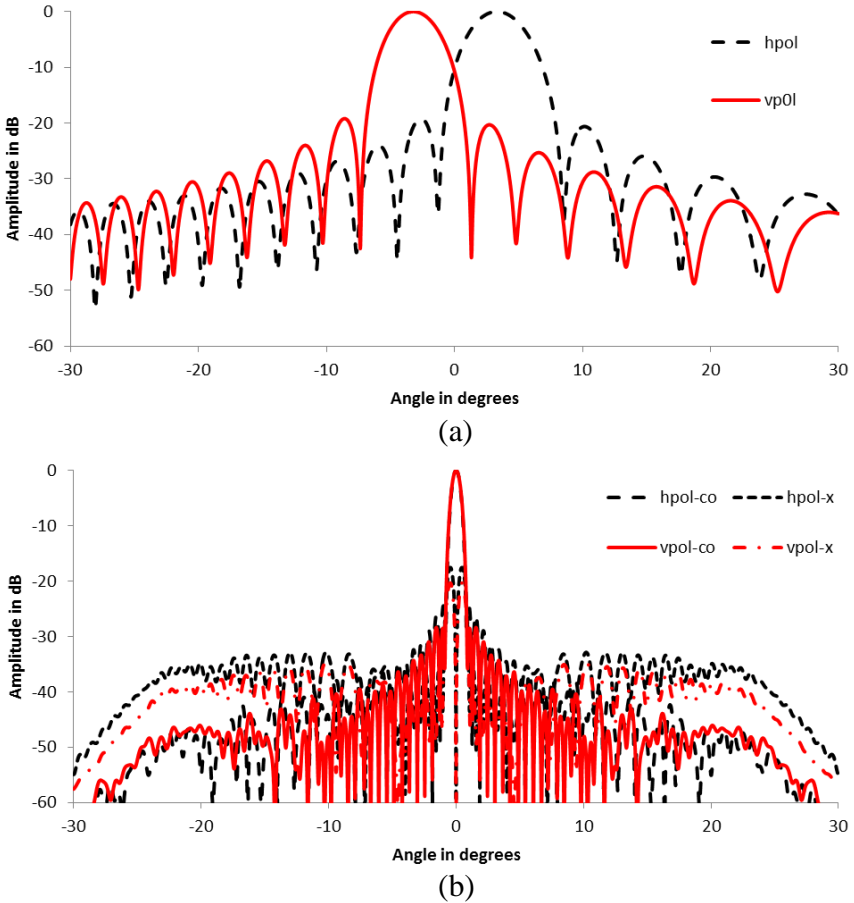


**Figure 5.** Far field patterns of a fully planar reflectarray with rectangular patches. (a) Elevation patterns. (b) Azimuth pattern.

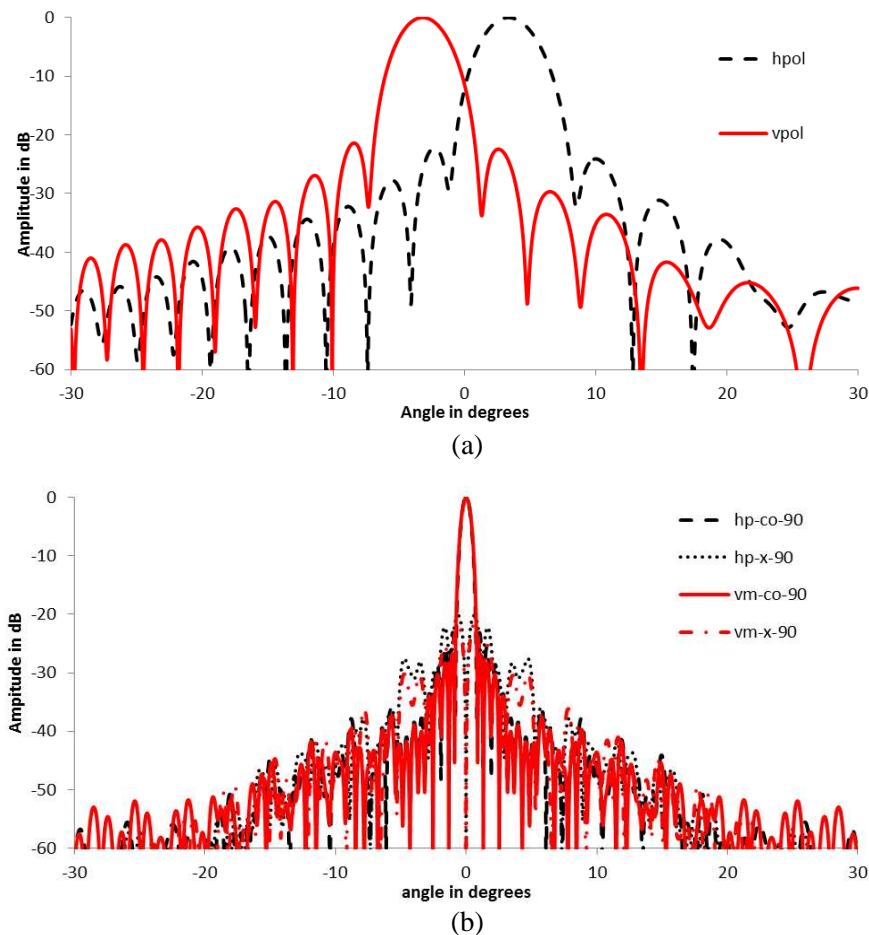


**Figure 6.** Far field patterns of a PPPR with 5 panels. (a) Elevation pattern. (b) Azimuth pattern.

thus validating the design technique for PPPR for dual-beam dual-polarization application. Results computed for the three-panel PPPR were very similar.

Figures 5 and 6 show far field patterns of fully planar reflectarray and PPPR consisting of rectangular patches. The pattern peaks are normalized to 0 dB for easy comparison of sidelobe and crosspol levels, even though PPPR have 0.1 to 0.2 dB higher gain values. There is no cross polarization in the elevation plane since it is a plane of symmetry. In the azimuth plane, hpol patterns exhibit greater levels of cross polarization and sidelobe levels, since h-pol beams are at larger oblique

**Table 8.** Gain in dB of the rectangular patch 5-panel PPPR designed for a feed at  $A$  and the orthogonally polarized feed at  $B$ .

Feed polarization	Designed for hpol at $A$ & vpol at $B$	Designed for vpol at $A$ & hpol at $B$
hpol	40.32	40.92
vpol	40.90	40.36

angles. The crosspol levels of PPPR are 1.5 to 2.5 dB better than those of the fully planar reflectarray. In the elevation plane, the sidelobe level of PPPR exhibits 1 to 2.5 dB lower levels than the corresponding values of the fully planar reflectarrays. Thus, in addition to providing improved bandwidth, PPPR provide better pattern performance as well.

#### 4. CONCLUSION

This paper has presented the results of a study of rectangular patch reflectarrays for nadir looking dual-beam dual-polarized radar interferometer applications. Fully planar rectangular patch reflectarrays provide an average of 0.4 dB improvement in gain compared to the square patch arrays by minimizing the gain variation with polarization. For PPPR in tilted configurations the design using square patches for the nominal feed position and then subsequent offsetting of the two feeds produces substantial gain loss. PPPR can be designed using rectangular patches for two simultaneous offset feeds with good patterns and gain values. Such an antenna eliminates the bandwidth limitation on the aperture size for large interferometric array applications and shows promise for use in many future space based deployable systems.

#### REFERENCES

1. Pozar, D. M., S. D. Targonski, and H. D. Syriogios, "Design of millimeter wave microstrip reflectarrays," *IEEE Transactions on Antennas and Propagation*, Vol. 45, No. 2, 287–296, Feb. 1997.
2. Hodges, R. E. and M. Zawadzki, "A reflectarray antenna for use in interferometric ocean height measurement," *IEEE Aerospace Conference*, 1131–1139, Big Sky, MT, Mar. 2005.
3. Zawadzki, M., S. R. Rengarajan, and R. E. Hodges, "The design of H- and V-pol slot array feeds for a scanned, offset,

- dual-polarized reflectarray,” *IEEE International Antennas and Propagation Symposium*, Washington, DC, Jul. 2005.
4. Esteban-Fernandez, D., et al., “KA band SAR interferometry studies for the SWOT mission,” *Proc. IEEE International Geoscience and Remote Sensing Symposium*, 4401–4402, 2010.
  5. Encinar, J. A. and M. Barba, “Design manufacture and test of ka band reflectarray antenna for transmitting and receiving orthogonal polarization,” *Proc. 14th International Symposium on Antenna Technology and Applied Electromagnetics (ANTEM) and the American Electromagnetics Conference (AMREM)*, 2010.
  6. Encinar, J. A., et al., “Dual-polarization dual-coverage reflectarray for space application,” *IEEE Transactions on Antennas and Propagation*, Vol. 54, No. 10, 2827–2837, Oct. 2006.
  7. Roederer, A., “Reflector antenna comprising a plurality of panels,” US Patent, No. US 2001/0020914 A1, Sep. 13, 2001.
  8. Legay, H., et al., “Reflectarrays for contoured beam antennas in Ku band,” *ESTEC Antenna Workshop*, 2010.
  9. Racette, P. E., et al., “A novel reflector/reflectarray antenna,” [http://esto.nasa.gov/conferences/estf2011/papers/Racette\\_EST-F2011.pdf](http://esto.nasa.gov/conferences/estf2011/papers/Racette_EST-F2011.pdf).
  10. Rengarajan, S. R., “Reciprocity considerations in microstrip reflectarrays,” *IEEE Antennas and Wireless Propagation Letters*, Vol. 8, 1206–1209, 2009.
  11. Rengarajan, S. R., “Choice of basis functions for accurate characterization of infinite array of microstrip reflectarrays,” *IEEE Antennas and Wireless Propagation Letters*, Vol. 4, 47–50, 2005.
  12. Rengarajan, S. R., “Scanning and defocusing characteristics of microstrip reflectarrays,” *IEEE Antennas and Wireless Propagation Letters*, Vol. 9, 163–166, 2010.
  13. Zhou, M., S. B. Sorenson, E. Jorgenson, P. Meincke, O. S. Kim, and O. Breinbjerg, “An accurate technique for calculation of radiation from printed reflectarrays,” *IEEE Antennas and Wireless Propagation Letters*, Vol. 10, 1081–1084, 2011.
  14. Pozar, D. M., “Bandwidth of reflectarrays,” *Electronics Letters*, Vol. 39, No. 11, 1490–1491, Oct. 16, 2003.
  15. Rahmat-Samii, Y., “Useful coordinate transformations for antenna applications,” *IEEE Transactions on Antennas and Propagation*, Vol. 27, No. 4, 571–572, Jul. 1979.
  16. Baars, J. W. M., *The Paraboloidal Reflector Antenna in Radio Astronomy and Communication*, Springer, New York, 2007.